Synthetic Anti-PT Symmetry in a Single Microcavity

Fangxing Zhang,[1] Yaming Feng,[2] Xianfeng Chen,[2] Li Ge,[3,*] and Wenjie Wan[1,2,†]
[1]The State Key Laboratory of Advanced Optical Communication Systems and Networks, University of Michigan-Shanghai Jiao Tong University Joint Institute, Shanghai Jiao Tong University, Shanghai 200240, China
[2]MOE Key Laboratory for Laser Plasmas and Collaborative Innovation Center of IFSA, Department of Physics and Astronomy, Shanghai Jiao Tong University, Shanghai 200240, China
[3]Department of Physics and Astronomy, College of Staten Island, the City University of New York, NY 10314, and the Graduate Center, CUNY, New York, New York 10016, USA

(Received 7 July 2019; revised manuscript received 31 December 2019; accepted 9 January 2020; published 3 February 2020)

Non-Hermitian systems based on parity-time (PT) and anti-PT symmetry reveal rich physics beyond the Hermitian regime. So far, realizations of such symmetric systems have been limited to the spatial domain. Here we theoretically and experimentally demonstrate synthetic anti-PT symmetry in a spectral dimension induced by nonlinear Brillouin scattering in a single optical microcavity, where Brillouin scattering induced transparency or absorption in two spectral resonances provides the optical gain and loss to observe a phase transition between two symmetry regimes. This scheme provides a new paradigm towards the investigation of non-Hermitian physics in a synthetic photonic dimension for all-optical signal processing and quantum information science.

DOI: 10.1103/PhysRevLett.124.053901

The operator description of quantum mechanics, formulated by Dirac and von Neumann, postulated that all physical observables are real valued and associated with a Hermitian operator, including the energy and its operator, the Hamiltonian. However, Bender and colleagues theoretically demonstrated in 1998 [1] that a new class of non-Hermitian Hamiltonians can possess a real energy spectrum below a certain phase-transition point, immediately opening up an opportunity for exploring interesting consequences of non-Hermitian physics. These systems are characterized by parity-time (PT) symmetry, with a complex potential $V(x)$ subject to the spatial-symmetry constraint $V(x) = V^*(-x)$. They undergo a phase transition near an "exceptional point," which signals the spontaneous breaking of PT symmetry and turns the real energy spectrum into a complex one. Ten years later, Christodoulides and collaborators proposed and experimentally realized such PT symmetry in optics [2], by utilizing the analogy between the Schrödinger equation in quantum mechanics and the paraxial optical diffraction equation.

A closely related symmetry, known as antisymmetric PT symmetry or anti-PT for short, was proposed by Ge and Türeci in optics that broadened the family of non-Hermitian symmetries [3]. Because of the definition of parity as a spatial operator, both PT and anti-PT symmetry were achieved by spatially arranging the effective optical potential. In the case of PT symmetry, it requires modulating the optical refractive index with properly balanced gain and loss spatial profiles. A model system consists of a pair of coupled waveguides, which have an identical real part and opposite imaginary parts of the refractive index [4]. Similarly arranged PT-symmetric systems have led to a plethora of discoveries [5], including unusual laser behaviors [6–8] and applications [9–12], anisotropic transmission resonances and unidirectional invisibility [13–15], robust wireless power transfer [16], and the coexistence of coherent perfect absorption and lasing [17–19]. In like manner, anti-PT symmetry has been demonstrated using spatially coupled flying atom beams [20], electrical circuits [21], and optical waveguides [22] with imaginary couplings.

To go beyond the original definition of PT and anti-PT symmetry, there has been theoretical work extending the definition of the parity operator [23] in the context of non-Hermitian Hamiltonians, e.g., to embrace any linear operator including rotation and inversion [24]. However, such generalized symmetries and their exceptional points have not been observed experimentally. The importance of utilizing such a "synthetic parity operator" lies in a broader scope of non-Hermitian physics based on PT and anti-PT symmetry, which offers a more versatile approach beyond a spatially arranged optical potential. Indeed, a related concept proposed by Fan and co-workers [25], i.e., the synthetic dimension in photonics, has opened a new territory for investigating optical effective gauge fields [26] and topological photonics [27,28].

Synthetic dimensions have been studied in other branches of physics, for example, using nuclear spins [29] and atomic spins [30] in condensed matter systems. Here this additional, synthetic dimension is enabled by coupling modes with different frequencies or angular momenta, achieved by imposing direct temporal modulation in resonant structures such as a whispering-gallery-mode (WGM) optical

microcavity [31]. Besides this "external" modulation approach, it is also well known that light can be converted into other frequencies in these microcavities through resonance-enhanced nonlinearities, including stimulated Raman scattering [32], Brillouin scattering [33], four-wave mixing [34] and optomechanical oscillations [35]. This "internal" modulation approach offers a new route to realize a synthetic frequency dimension [36], which has led to the observation of some striking photonic dynamics, e.g., optically induced transparency and slow light [37,38]. It remains a big challenge to realize non-Hermitian photonics with the synthetic dimension in microcavities, and it has yet to be demonstrated. For this purpose, it is highly desired to replace the spatial parity in prior works with two-coupled microcavities [39,40] and synthesize an additional frequency domain through nonlinear conversion, for a new platform to investigate non-Hermitian physics.

In this work, we theoretically and experimentally demonstrate synthetic anti-PT symmetry in this synthetic spectral dimension using one single optical microcavity. Unlike previous explorations of the original PT and anti-PT symmetry, here two *spectrally* separated optical resonances in a *single* microcavity are coupled by nonlinear frequency conversion through stimulated Brillouin scattering (SBS), without the need of having a second microcavity in the spatial PT case. These two nonlinear-coupled resonances can interfere with each other and result in either electromagnetically induced transparency (EIT) or absorption (EIA), similar to their counterparts in atomic physics. By using a detuning technique developed specifically for this framework, we are able to observe a striking non-Hermitian phase transition at an exceptional point. These results expand the scope of non-Hermitian photonics into the synthetic spectral dimension, providing a new paradigm to exploit the benefits of PT and anti-PT symmetry.

Our proposed spectral anti-PT symmetric system is shown schematically in Fig. 1. Here an incident probe wave at the frequency ω_p propagates from left to right (forward) in a tapered fiber and evanescently tunnels into the neighboring microsphere resonator. By sweeping its frequency at low power, clockwise (CW) WGM resonances can be excited sequentially. The resulting dips in the transmission spectrum [Fig. 1(b), top; without the sharp BSIA dip on the right] are given by inverted Lorentzians well separated from each other, indicating no nonlinear coupling between them. However, if the power of the probe increases above a certain threshold, it can stimulate the generation of Stokes photons at a lower frequency ω_s and coherent acoustical phonons at frequency $\Omega = \omega_p - \omega_s$ through an electrostrictive-induced SBS process [41]. This process has a low threshold if $\omega_{p,s}$ and Ω_B are close to their respective optical and acoustic WGM resonances [33]. In our experiment, the Stokes photons are confined in a counterclockwise (CCW) WGM mode [Fig. 1(a)] to fulfill the conservation law of momentum. The induced Brillouin dynamical grating (BDG) [42] from the generated acoustical wave now mediates the nonlinear coupling between the two optical resonances involved, providing the needed non-Hermitian feature to realize synthetic PT and anti-PT symmetry [Fig. 1(c)].

To keep a stable nonlinear coupling between the probe and Stokes photons while sweeping the probe frequency,

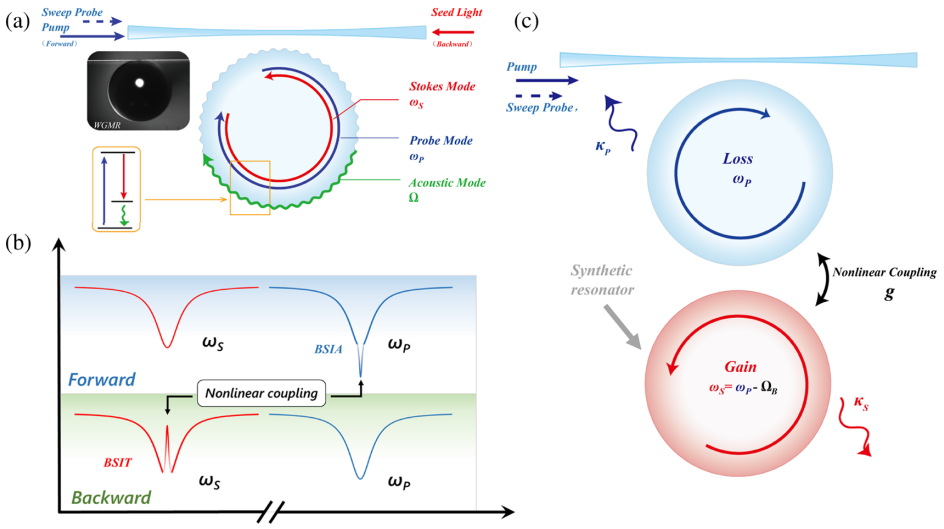

FIG. 1. Conceptual illustration of a synthetic anti-PT-symmetric optical microcavity. (a) Nonlinear Brillouin scattering in a WGM microcavity with two optical modes, i.e., the probe and Stokes modes, together with an acoustic mode. Lower inset: Energy transition diagram. Upper inset: SEM of one high-Q microsphere microcavity coupled to the tapered fiber. (b) Nonlinear gain and loss processes manifested as BSIT and BSIA in the transmission spectra. The BSIT peak and the BSIA dip need to be measured separated using a probe in the backward and forward direction, respectively. (c) Schematics showing the synthetic PT symmetry along the frequency dimension. $\kappa_{p,s}$ are the linear losses of the probe and Stokes modes.

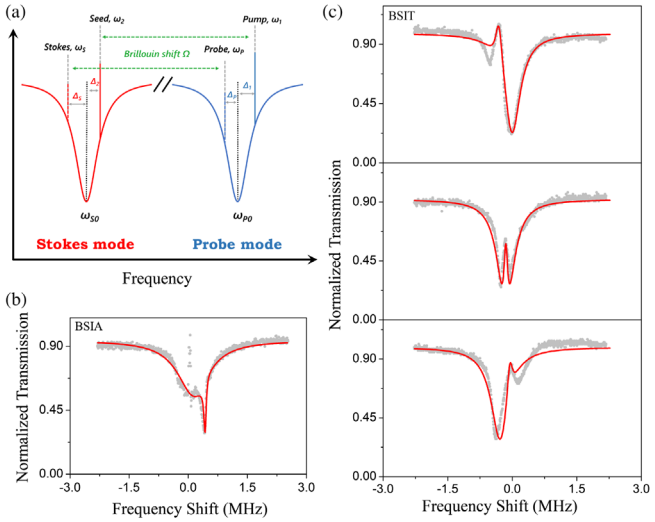

FIG. 2. Brillouin scattering induced transparency and absorption in a synthetic anti-PT-symmetric microcavity. (a) Illustration of the pump-seed setup in the experimental, where a strong pump beam at ω_1 and a seed at ω_2 are launched to induce a Brillouin dynamic grating. A weak probe in the forward direction is used to measure the BSIA near the pump (b) and synthetic anti-PT breaking (Fig. 3). In a separate experiment, a backward probe is used instead to scan near the seed frequency (c), which demonstrates the tuning of the phonon frequency via the pump-seed controlled BDG.

we, in fact, use a strong pair of the pump at ω_1 close to ω_p [Fig. 2(a)] and the seed at ω_2 near ω_s to lock the BDG, which allows us to control the frequency of the generated acoustic phonons (details to be elucidated later). Here to discuss the synthetic anti-PT symmetry of the probe and Stokes waves, the dynamics of the strong pump and seed can be eliminated [43], leading to a coupled-mode theory for the amplitudes of the probe wave (A_p) and Stokes wave (A_s) in the microsphere:

$$\begin{aligned} i\frac{\partial A_p}{\partial t} &= (-i\kappa_p - \Delta_p)A_p - gA_s, \\ i\frac{\partial A_s}{\partial t} &= (-i\kappa_s - \Delta_s)A_s + g^*A_p. \end{aligned} \tag{1}$$

Here we emphasize that the subscripts p (probe) and s (Stokes) do not stand for the pump and the signal, contrary to the standard notation in three-wave mixing processes. $\kappa_{p,s}$ are their respective cavity decay rates due to internal absorption, scattering, radiation loss, and external coupling, which we take to be the same for simplicity. $\Delta_{p,s} = \omega_{p,s} - \omega_{p0,s0}$ are the frequency detunings from their neighboring WGM frequencies (denoted by $\omega_{p0,s0}$), which are related by $\Delta_p - \Delta_s = \Omega - (\omega_{p0} - \omega_{s0})$. Δ_p is controlled directly by scanning the probe frequency, while Δ_s is tuned indirectly by changing the seed frequency via the SBS generated phonons at frequency $\Omega = \omega_1 - \omega_2 g$. The most crucial coupling term can also be controlled by the strength of the BDG [43].

As we mentioned before, the standard PT symmetry in optics is satisfied by coupling two or more optical modes in spatially separated resonators or waveguides with different effective gain and loss. Using the simplest case without losing generality, the non-Hermitian Hamiltonian can be written as a 2×2 matrix in the basis of two uncoupled modes [4]:

$$H_{\mathrm{PT}} = \begin{bmatrix} i\gamma & \kappa \\ \kappa & -i\gamma \end{bmatrix}. \tag{2}$$

Here the gain and loss parameter γ and the linear coupling κ are both real, and the parity operator P is a mirror reflection given by the first Pauli matrix σ_x, which exchanges the spatial positions of these two optical modes. The PT symmetry is evident through the relation $[H_{\mathrm{PT}}, \mathrm{PT}] = 0$, where the time-reversal operator T is given by the complex conjugation.

To compare Eq. (1) to this standard PT Hamiltonian, we rewrite it in the basis $A_p = a_p e^{i(\Delta + i\kappa_p)t}$, $A_s = a_s e^{i(\Delta + i\kappa_s)t}$:

$$i\frac{\partial}{\partial t}\begin{pmatrix} a_p \\ a_s \end{pmatrix} = \begin{pmatrix} -\delta & -g \\ g^* & \delta \end{pmatrix}\begin{pmatrix} a_p \\ a_s \end{pmatrix} \equiv H_s \begin{pmatrix} a_p \\ a_s \end{pmatrix}, \tag{3}$$

where $\Delta \equiv (\Delta_p + \Delta_s)/2$ is the average detuning and $\delta = (\Delta_p - \Delta_s)/2$. Unlike H_{PT}, there is no explicit gain or loss in this non-Hermitian Hamiltonian; the effective loss to the probe photons and effective gain to the Stokes wave are represented inexplicitly by the off-diagonal nonlinear coupling terms. Therefore, it is clear that H_s does not commute with the original PT operator mentioned above.

Interestingly, H_s displays anti-PT symmetry under the traditional PT operator, i.e., it satisfies the anticommutation relation $\{H_s, \mathrm{PT}\} = 0$. We note that this property is achieved without resorting to an imaginary coupling in previous demonstrations of anti-PT symmetry in the spatial domain [20–22]. Since now $P = \sigma_x$ exchanges the spectral position of the probe wave and its Stokes wave in the same cavity, we will refer to this symmetry as a synthetic anti-PT symmetry. In the meanwhile, it can also be shown that H_s satisfies a generalized PT symmetry $[H_s, P_s T] = 0$ simultaneously, with a synthetic parity operator defined by

$$P_s = \frac{ig_r\sigma_y + \delta\sigma_z}{\sqrt{\delta^2 - g_r^2}}. \tag{4}$$

Here $\sigma_{y,z}$ are the other two Pauli matrices, $g_r = \mathrm{Re}[g]$, and the denominator is introduced to satisfy $(P_s T)^2 = 1$. In fact, H_s is pseudo-Hermitian [48], satisfying $\eta^{-1} H_S \eta = H_S^\dagger$ with $\eta = \sigma_z$.

The two eigenvalues of H_s are given by

$$\lambda_{\pm} = \pm\sqrt{\delta^2 - |g|^2}. \tag{5}$$

Obviously, when $|\Delta_p - \Delta_s| = 2|\delta| > 2|g|$, these two eigenvalues are real and different, resulting in two spectrally separated resonances. It is important to note that they are not the two optical WGM modes in the rotating frame. Instead, they indicate that the probe and the Stokes wave inside the cavity now hybridize to form two dynamical eigenmodes $\Psi_{\pm}$, one with mixed frequencies $\omega_{p0,s0} + \Delta + \sqrt{\delta^2 - |g|^2}$ and the other $\omega_{p0,s0} + \Delta - \sqrt{\delta^2 - |g|^2}$. The phenomenon is independent of our pump-seed scheme and would occur if we excite the acoustic phonons mechanically to induce the BDG. Since in this regime the eigenvectors representing $\Psi_{\pm}$ transform back into themselves under the synthetic P_sT operation and into each other under the PT operation that defines the anti-PT symmetry, we will refer to this regime as the unbroken PT phase and broken-anti-PT phase. This coexistence of broken and unbroken phases is similar to systems with simultaneous PT and non-Hermitian particle-hole symmetry [49].

The system is in the PT-broken and unbroken-anti-PT phase when $|\Delta_p - \Delta_s| < 2|g|$. The two eigenfrequencies $\lambda_{\pm}$ are now complex conjugates, with the same real part (spectral center) but different imaginary parts (decay rates). $|\Delta_p - \Delta_s| = 2|g|$ gives the exceptional point of both synthetic PT and anti-PT symmetry, where the two hybrid dynamical eigenmodes (instead of the two optical WGMs) become identical. This different implication of an exceptional point distinguishes our nonlinear and non-Hermitian system from its linear counterparts.

Experimentally, we first investigate the nonlinear coupling induced gain and loss near the probe and its Stokes resonance. Under the steady-state condition, the transmission spectra of the probe in the forward direction in the fiber and that of the Stokes resonance in the backward direction can be derived from Eq. (1) to show occurrences of BSIT and BSIA in Fig. 2[43]. They arise from the interference between the probe and Stokes resonances through a nonlinear coupling. Take the BSIT, for example [Fig. 2(c)]. The narrow gain peak induced near the Stokes resonance (in the backward direction) is enhanced by the optical resonance at the pump frequency through a BS process, which has a relatively broad spectral width ~30 MHz (inversely proportional to acoustic lifetime) [41] and wider than the optical resonance ~1 MHz in our experiment. BSIT or BSIA under such a broad gain bandwidth was considered unlikely, but we note that nonlinear coupling, in fact, narrows the gain linewidth resonantly to be on the order of the optical resonance, similar to an FWM enabled optically induced transparency we have demonstrated previously [34]. Similar spectral profiles can be found in the probe's BSIA transmission in the forward direction near the pump resonance as shown in Fig. 2(b), where the induced absorption dip also has similar linewidth as its optical resonance. These results validate the nonlinear coupling between the probe and its Stokes resonance, offering us a synthetic platform to realize anti-PT symmetry.

To observe synthetic anti-PT symmetry breaking, we vary the two detuning factors $\Delta_{p,s}$ systematically. This approach is very different from the investigations of the standard PT symmetry in twin-coupled microcavities [39,40], where the detuning between the two optical resonances, one in each microcavity, needs to be avoided by all means to achieve anti-PT symmetry. Because both the pump-seed pair and the probe-Stokes pair are related through the SBS generated phonons, i.e., $\omega_1 - \omega_2 = \omega_p - \omega_s = \Omega$ [see Fig. 2(a)], the critical parameter $|\Delta_p - \Delta_s|$ for synthetic anti-PT symmetry breaking is equal to $|\Omega - (\omega_{p0} - \omega_{s0})|$. Therefore, this critical parameter is tuned only by the seed frequency in our pump-seed scheme with a fixed pump frequency and does not actually depend on the probe frequency. We use the latter property to our advantage: for each seed frequency, we can then map out the central frequencies and linewidths of the two dynamical modes predicted by Eq. (4) by simply scanning close to the pump frequency.

In Figs. 2(c)–2(e), we show the tuning of the induced transparency window near the Stokes mode (i.e., Δ_s) by detuning the seed beam in our pump-seed scheme, which is both effective and systematic. Note that when $|\Delta_s|$ is large, this peak evolves into an asymmetric Fano line shape [Fig. 2(c)] similar to prior works [34]. In the meantime, we do not observe any visible shift of the BSIA spectrum in Fig. 2(b), because it highly depends on the strong pump's detuning fixed during the whole measurement.

The breaking of synthetic anti-PT symmetry in our system is observed using a lock-in amplification technique [43] on the probe beam, which can detect the presence of any dynamical mode predicted by Eq. (5). Meanwhile, we manage to precisely tune the seed beam in order to control $|\Delta_p - \Delta_s|$ and keep a relatively constant $|g|$. During this tuning process, both $\Delta_{p,s}$ and the effective gain $|g|$ are calibrated in Ref. [43]. Initially,the two modes represented by $\lambda_{\pm}$ in Eq. (5) are split by about 0.6 MHz under the condition $|(\Delta_p - \Delta_s)/g| \approx 12$. As the ratio becomes smaller in the unbroken anti-PT phase, so does the frequency difference of the two dynamical modes [Fig. 3(b)], which agrees well with the theoretical prediction given by Eq. (5). Meanwhile, the linewidths of both modes maintain a constant value [Fig. 3(c)], also agreeing with Eq. (5). Physically, the effective nonlinear gain is not strong enough to compete with the cavity loss such that two modes are relatively independent. However, as the detuning factor gradually reduces to $|\Delta_p - \Delta_s| \approx 2|g|$, i.e., the exceptional

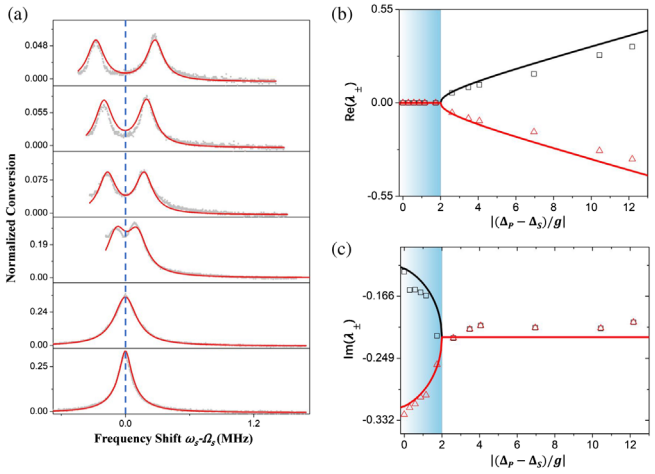

FIG. 3. Experimental observation of synthetic anti-PT symmetry breaking. (a) Spectral evolution of the probe conversion to its Stokes wave by tuning the phonon frequency of BDG. Ω_s is the unsplit frequency defined as $\Omega_s = (\omega_{p0} + \omega_{s0} - \Omega)/2$ [43]. The pump and seed lasers are fixed at 15.22 mW and 69.4 μW, respectively, while the power of the weak probe is 3.48 μW. The real parts (b) and imaginary parts (c) of the dynamical eigenfrequencies measured in the synthetic anti-PT system. The exceptional point at $|(\Delta_p - \Delta_s)/g| = 2$ marks the phase transition boundary. The solid lines are obtained from the theoretical model in Eq. (5).

point, the two split modes begin to merge into one single mode, where the frequency splitting vanishes [Fig. 3(b)]. Above the EP, the two modes remain aligned but differ in their linewidths, which can be extracted from Fig. 3(a) using the superposition of two Lorentzian line shapes. The measured result again verifies the prediction of Eq. (5), which completes our demonstration of a synthetic anti-PT symmetry breaking in a single microcavity.

In conclusion, we have realized anti-PT symmetry in a synthetic spectral dimension and observed its spontaneous breaking using nonlinear Brillouin scattering in a single optical microcavity. Our work opens a new frontier at the junction of two emerging fields in physics, namely, synthetic dimension and non-Hermitian physics based on PT symmetry. Our results also offer a unique perspective on the relationship between non-Hermitian physics and nonlinear optical processes, which can be extended to investigate a wide range of phenomena including second-harmonic generation, parametric amplification [50], and four-wave mixing [51,52].

This work was supported by the National Key Research and Development Program (Grants No. 2016YFA0302500, No. 2017YFA0303700); National Science Foundation of China (Grants No. 11674228, No. 11304201, No. 61475100); Shanghai MEC Scientific Innovation Program (Grant No. E00075) and NSF (Grant No. PHY-1847240).

*Corresponding author.
wenjie.wan@sjtu.edu.cn
†Corresponding author.
li.ge@csi.cuny.edu

[1] M. Bender and S. Boettcher, Real Spectra in Non-Hermitian Hamiltonians Having PT Symmetry, Phys. Rev. Lett. **80**, 5243 (1998).
[2] A. Guo, G. Salamo, D. Duchesne, R. Morandotti, M. Volatier-Ravat, V. Aimez, G. Siviloglou, and D. Christodoulides, Observation of PT-Symmetry Breaking in Complex Optical Potentials, Phys. Rev. Lett. **103**, 093902 (2009).
[3] L. Ge and H. E. Türeci, Antisymmetric PT-photonic structures with balanced positive-and negative-index materials, Phys. Rev. A **88**, 053810 (2013).
[4] C. E. Rüter, K. G. Makris, R. El-Ganainy, D. N. Christodoulides, M. Segev, and D. Kip, Observation of parity–time symmetry in optics, Nat. Phys. **6**, 192 (2010).
[5] L. Feng, R. El-Ganainy, and L. Ge, Non-Hermitian photonics based on parity–time symmetry, Nat. Photonics **11**, 752 (2017).
[6] M. Liertzer, L. Ge, A. Cerjan, A. Stone, H. Türeci, and S. Rotter, Pump-Induced Exceptional Points in Lasers, Phys. Rev. Lett. **108**, 173901 (2012).
[7] R. El-Ganainy, M. Khajavikhan, and L. Ge, Exceptional points and lasing self-termination in photonic molecules, Phys. Rev. A **90**, 013802 (2014).
[8] B. Peng, Ş. Özdemir, S. Rotter, H. Yilmaz, M. Liertzer, F. Monifi, C. Bender, F. Nori, and L. Yang, Loss-induced suppression and revival of lasing, Eng. Sci. Mech. **346**, 328 (2014).
[9] P. Miao, Z. Zhang, J. Sun, W. Walasik, S. Longhi, N. M. Litchinitser, and L. Feng, Orbital angular momentum microlaser, Science **353**, 464 (2016).
[10] J. Wiersig, Enhancing the Sensitivity of Frequency and Energy Splitting Detection by Using Exceptional Points: Application to Microcavity Sensors for Single-Particle Detection, Phys. Rev. Lett. **112**, 203901 (2014).
[11] W. Chen, Ş. K. Özdemir, G. Zhao, J. Wiersig, and L. Yang, Exceptional points enhance sensing in an optical microcavity, Nature (London) **548**, 192 (2017).
[12] H. Hodaei, A. U. Hassan, S. Wittek, H. Garcia-Gracia, and M. Khajavikhan, Enhanced sensitivity at higher-order exceptional points, Nature (London) **548**, 187 (2017).
[13] L. Ge, Y. Chong, and A. D. Stone, Conservation relations and anisotropic transmission resonances in one-dimensional PT-symmetric photonic heterostructures, Phys. Rev. A **85**, 023802 (2012).
[14] L. Feng, Y.-L. Xu, W. S. Fegadolli, M.-H. Lu, J. E. Oliveira, V. R. Almeida, Y.-F. Chen, and A. Scherer, Experimental demonstration of a unidirectional reflectionless parity-time metamaterial at optical frequencies, Nat. Mater. **12**, 108 (2013).
[15] Z. Lin, H. Ramezani, T. Eichelkraut, T. Kottos, H. Cao, and D. N. Christodoulides, Unidirectional Invisibility Induced by PT-Symmetric Periodic Structures, Phys. Rev. Lett. **106**, 213901 (2011).
[16] S. Assawaworrarit, X. Yu, and S. Fan, Robust wireless power transfer using a nonlinear parity–time-symmetric circuit, Nature (London) **546**, 387 (2017).

[17] S. Longhi, PT-symmetric laser absorber, Phys. Rev. A **82**, 031801(R) (2010).
[18] Y. D. Chong, L. Ge, and A. D. Stone, PT-Symmetry Breaking and Laser-Absorber Modes in Optical Scattering Systems, Phys. Rev. Lett. **106**, 093902 (2011).
[19] J.-w. Deng, U. Guenther, and Q.-h. Wang, General PT-symmetric matrices, arXiv:1212.1861.
[20] P. Peng, W. Cao, C. Shen, W. Qu, J. Wen, L. Jiang, and Y. Xiao, Anti-parity–time symmetry with flying atoms, Nat. Phys. **12**, 1139 (2016).
[21] Y. Choi, C. Hahn, J. W. Yoon, and S. H. Song, Observation of an anti-PT-symmetric exceptional point and energy-difference conserving dynamics in electrical circuit resonators, Nat. Commun. **9**, 2182 (2018).
[22] X.-L. Zhang, T. Jiang, and C. T. Chan, Dynamically encircling an exceptional point in anti-parity-time symmetric systems: Asymmetric mode switching for symmetry-broken modes, Light Sci. Appl. **8**, 1 (2019).
[23] C. M. Bender, P. N. Meisinger, and Q. Wang, All Hermitian Hamiltonians have parity, J. Phys. A **36**, 1029 (2003).
[24] L. Ge and A. D. Stone, Parity-Time Symmetry Breaking Beyond One Dimension: The Role of Degeneracy, Phys. Rev. X **4**, 031011 (2014).
[25] L. Yuan, Q. Lin, M. Xiao, and S. Fan, Synthetic dimension in photonics, Optica **5**, 1396 (2018).
[26] L. Yuan, Y. Shi, and S. Fan, Photonic gauge potential in a system with a synthetic frequency dimension, Opt. Lett. **41**, 741 (2016).
[27] Q. Lin, M. Xiao, L. Yuan, and S. Fan, Photonic Weyl point in a two-dimensional resonator lattice with a synthetic frequency dimension, Nat. Commun. **7**, 13731 (2016).
[28] A. Dutt, Q. Lin, L. Yuan, M. Minkov, M. Xiao, and S. Fan, A single photonic cavity with two independent physical synthetic dimensions, Science **367**, 59 (2020).
[29] M. Mancini *et al.*, Observation of chiral edge states with neutral fermions in synthetic Hall ribbons, Science **349**, 1510 (2015).
[30] B. Stuhl, H.-I. Lu, L. Aycock, D. Genkina, and I. Spielman, Visualizing edge states with an atomic Bose gas in the quantum Hall regime, Science **349**, 1514 (2015).
[31] K. J. Vahala, Optical microcavitiesl, Nature (London) **424**, 839 (2003).
[32] S. Spillane, T. Kippenberg, and K. Vahala, Ultralow-threshold Raman laser using a spherical dielectric microcavity, Nature (London) **415**, 621 (2002).
[33] G. Bahl, J. Zehnpfennig, M. Tomes, and T. Carmon, Stimulated optomechanical excitation of surface acoustic waves in a microdevice, Nat. Commun. **2**, 403 (2011).
[34] Y. Zheng, J. Yang, Z. Shen, J. Cao, X. Chen, X. Liang, and W. Wan, Optically induced transparency in a micro-cavity, Light Sci. Appl. **5**, e16072 (2016).
[35] T. J. Kippenberg and K. J. Vahala, Cavity opto-mechanics, Opt. Express **15**, 17172 (2007).
[36] B. A. Bell, K. Wang, A. S. Solntsev, D. N. Neshev, A. A. Sukhorukov, and B. J. Eggleton, Spectral photonic lattices with complex long-range coupling, Optica **4**, 1433 (2017).
[37] J. H. Kim, M. C. Kuzyk, K. Han, H. Wang, and G. Bahl, Non-reciprocal brillouin scattering induced transparency, Nat. Phys. **11**, 275 (2015).
[38] C.-H. Dong, Z. Shen, C.-L. Zou, Y.-L. Zhang, W. Fu, and G.-C. Guo, Brillouin-scattering-induced transparency and non-reciprocal light storage, Nat. Commun. **6**, 6193 (2015).
[39] B. Peng, Ş. K. Özdemir, F. Lei, F. Monifi, M. Gianfreda, G. L. Long, S. Fan, F. Nori, C. M. Bender, and L. Yang, Parity–time-symmetric whispering-gallery microcavities, Nat. Phys. **10**, 394 (2014).
[40] L. Chang, X. Jiang, S. Hua, C. Yang, J. Wen, L. Jiang, G. Li, G. Wang, and M. Xiao, Parity–time symmetry and variable optical isolation in active–passive-coupled microresonators, Nat. Photonics **8**, 524 (2014).
[41] R. W. Boyd, *Nonlinear Optics* (Academic Press, 2010), 3rd ed., pp. 436–441.
[42] Y. Feng, F. Zhang, Y. Zheng, L. Chen, D. Shen, W. Liu, and W. Wan, Coherent control of acoustic phonons by seeded Brillouin scattering in polarization-maintaining fibers, Opt. Lett. **44**, 2270 (2019).
[43] See Supplemental Material at http://link.aps.org/supplemental/10.1103/PhysRevLett.124.053901 for both the experimental and theoretical details, which includes Refs. [44–47].
[44] G. Agarwal and S. S. Jha, Multimode phonon cooling via three-wave parametric interactions with optical fields, Phys. Rev. A **88**, 013815 (2013).
[45] D. Marcuse, Coupled mode theory of optical resonant cavities, IEEE J. Quantum Electron. **21**, 1819 (1985).
[46] K. Y. Song, W. Zou, Z. He, and K. Hotate, All-optical dynamic grating generation based on Brillouin scattering in polarization-maintaining fiber, Opt. Lett. **33**, 926 (2008).
[47] A. Scott and K. Ridley, A review of Brillouin-enhanced four-wave mixing, IEEE J. Quantum Electron. **25**, 438 (1989).
[48] A. Mostafazadeh, Pseudo-Hermiticity versus PT symmetry: The necessary condition for the reality of the spectrum of a non-Hermitian Hamiltonian, J. Math. Phys. (N.Y.) **43**, 205 (2002).
[49] L. Ge, Symmetry-protected zero-mode laser with a tunable spatial profile, Phys. Rev. A **95**, 023812 (2017).
[50] R. El-Ganainy, J. I. Dadap, and R. M. Osgood, Optical parametric amplification via non-Hermitian phase matching, Opt. Lett. **40**, 5086 (2015).
[51] L. Ge and W. Wan, Pseudo-Hermitian transition in degenerate nonlinear four-wave mixing, arXiv:1603.05624.
[52] Y. Jiang, Y. Mei, Y. Zuo, Y. Zhai, J. Li, J. Wen, and S. Du, Anti-Parity-Time Symmetric Optical Four-Wave Mixing in Cold Atoms, Phys. Rev. Lett. **123**, 193604 (2019).